

# Elastic Constants of Quantum Solids by Path Integral Simulations

Philipp Schöffel and Martin H. Müser  
*Institut für Physik, WA 331; Johannes Gutenberg-Universität  
55099 Mainz; Germany*  
(October 30, 2018)

Two methods are proposed to evaluate the second-order elastic constants of quantum mechanically treated solids. One method is based on path-integral simulations in the  $NVT$  ensemble using an estimator for elastic constants  $C_{ij}$ . The other method is based on simulations in the  $NpT$  ensemble exploiting the relationship between strain fluctuations and elastic constants. The strengths and weaknesses of the methods are discussed thoroughly. We show how one can reduce statistical and systematic errors associated with so-called primitive estimators. The methods are then applied to solid argon at atmospheric pressures and solid helium 3 (hcp, fcc, and bcc) under varying pressures. Good agreement with available experimental data on elastic constants is found for  $^3\text{He}$ . Predictions are made for the thermal expectation value of the kinetic energy of solid  $^3\text{He}$ .

PACS: 67.80.-s, 62.20.Dc, 02.70.Ns, 05.30.-d

## I. INTRODUCTION

The quantum nature of atomic motion alters thermal and mechanical properties of condensed matter at low temperatures. The most striking feature is the well-known quantum mechanical freezing of solids below the Debye temperature: Specific heat and thermal expansion vanish as the temperature approaches absolute zero<sup>1</sup>. This behavior is different from what we would expect from classical statistical mechanics. A “classical solid” typically has a positive expansion coefficient at low temperatures and a specific heat close to  $3k_B$  per atom.

Path integral Monte Carlo (PIMC)<sup>2–5</sup> and path integral molecular dynamics (PIMD)<sup>6,7</sup> are convenient numerical methods to predict the proper low-temperature properties of condensed matter, provided that model potentials are available that describe the interatomic interactions sufficiently well. So far, most PIMC and PIMD studies have been restricted to the calculation of structural and thermal properties of quantum solids or to the calculation of equations of state of condensed rare gases. The computation of the tensor of the elastic constants, which is an important material property in many engineering applications, however, has not been put forward yet in the framework of path-integral simulations.

The proper evaluation of the elastic constants is far more complicated than textbooks on solid state physics make us believe, because it is not sufficient to calculate second derivatives of interaction potentials at equilibrium (or thermal) positions and construct from this the various  $C_{ij}$ . As shown by Squire, Holt, and Hoover,<sup>8</sup> thermal fluctuations of a generalized strain tensor can alter elastic constants significantly. Of course, quantum fluctuations can be expected to result in a similar effect. These fluctuations vanish at small temperatures for classical systems, but they do not necessarily vanish for quantum mechanical systems. Another difficulty is that quantum solids do not adopt a configuration at  $T = 0$  K where the potential energy surface is minimized. Instead, the atoms also

probe non-harmonic parts of the potentials due to quantum fluctuations, typically leading to lattice constants that are slightly increased with respect to the equivalent classical system.

In this paper, we want to propose two methods which enable us to determine accurately elastic constants of solids such that quantum effects of the atomic motion are fully included in the treatment. One possibility is to use the definition of the elastic constants as the second derivative of the free energy with respect to strain tensor elements and evaluate the final expression in the  $NVT$  ensemble. This procedure is similar to the method proposed by Squire, Holt, and Hoover,<sup>8</sup> with the difference that our partition function is quantum mechanical. Alternatively, one can perform simulations in the  $NpT$  ensemble and relate the fluctuations of the strain tensor to the elastic constants as has been originally done by Parrinello and Rahman for classical systems.<sup>9</sup>

Both methods are prone to produce large statistical error bars. In classical simulations, the computation of elastic constants using the  $NpT$  ensembles is known to be much less efficient than in the  $NVT$  ensemble<sup>10</sup>. However, the estimator derived for the quantum simulations in the  $NVT$  ensemble can be expected to become unreliable when the Trotter number  $P$  in the path-integral simulation becomes large, just like the so-called primitive estimator for the kinetic energy<sup>11</sup>. It is thus necessary to discuss the prospective statistical errors in detail.

It is important to note that presently only isothermal quantum mechanical elastic constants can be calculated. Adiabatic elastic constants can only be obtained if simulations are carried out in the  $NVE$  ensemble or the  $NpH$  ensemble.<sup>9</sup> Constraining the energy  $E$  or the enthalpy  $H$  to constant values in the simulation does not necessarily correspond to conserved  $E$  or  $H$  of the real quantum system.

The remainder of this paper is organized as follows: In Sec. II, the equations are derived that allow the correct determination of all  $C_{ij}$  in the  $NVT$  ensemble in terms of a path integral formulation. In this context, we will give

an in depth discussion of the statistical errors that will arise as a consequence of the corrections to  $C_{ij}$  associated with the quantum mechanical kinetic energy. It will be shown, how, simple corrections to primitive estimators can reduce their statistical uncertainties considerably. We will also briefly review the method to determine  $C_{ij}$  in the  $NpT$  ensemble as well as the simulation algorithm that is used for the applications. In Sec. III, the methods will be applied to the calculation of elastic constants of solid Argon as well as of fcc, bcc, and, hcp  $^3\text{He}$ . In the case of  $^3\text{He}$ , the corrections to primitive estimators will also be used to make predictions for thermal expectation values of the kinetic energy. Conclusions are drawn in Sec. IV.

## II. THEORY

### A. Derivation of Elastic Constants

As pointed out correctly for classical systems<sup>8</sup>, isothermal elastic constants<sup>12</sup>  $C_{ij}$  are insufficiently described if they are evaluated solely on the basis of averaging the so-called Born contribution  $C_{ij}^{(\text{Born})}$

$$C_{ij}^{(\text{Born})} = \frac{1}{V} \left\langle \frac{\partial^2 V_{\text{pot}}}{\partial \epsilon_i \partial \epsilon_j} \right\rangle, \quad (1)$$

which is the thermal average of the second derivative of the potential energy  $V_{\text{pot}}$  with respect to strain tensor elements  $\epsilon_i$  and  $\epsilon_j$  in the  $NVT$  ensemble. The full elastic constants are obtained if  $\langle V_{\text{pot}} \rangle$  is replaced with the free energy  $F(N, V, T) = -k_B T \ln Z(N, V, T)$ , e.g.,

$$C_{ij} = -\frac{k_B T}{V} \frac{\partial^2 \ln Z(N, V, T)}{\partial \epsilon_i \partial \epsilon_j} \quad (2)$$

with  $Z(N, V, T)$  the isothermal partition function. This proper definition results in corrections to  $C_{ij}^{(\text{Born})}$ . The leading correction terms  $C_{ij}^{(\text{fluc})}$  are fluctuations of the (generalized) instantaneous strains. These terms have the form

$$C_{ij}^{(\text{fluc})} = \frac{\beta}{V} \left( \left\langle \frac{\partial V_{\text{pot}}}{\partial \epsilon_i} \right\rangle \left\langle \frac{\partial V_{\text{pot}}}{\partial \epsilon_j} \right\rangle - \left\langle \frac{\partial V_{\text{pot}}}{\partial \epsilon_i} \frac{\partial V_{\text{pot}}}{\partial \epsilon_j} \right\rangle \right), \quad (3)$$

where again the expectation values are evaluated in the  $NVT$  ensemble. As far as classical elastic constants are concerned, the only missing contributions  $C_{ij}^{(\text{kin})}$  to the correct  $C_{ij}$  stem from the ideal gas part of the partition function. These kinetic corrections are given by

$$C_{ij}^{(\text{kin})} = -\frac{Nk_B T}{V} \frac{\partial^2 \ln V}{\partial \epsilon_i \partial \epsilon_j} \quad (4)$$

or in tensor notation for cubic symmetry

$$C_{\alpha\beta\gamma\delta}^{(\text{kin})} = \frac{Nk_B T}{V} \delta_{\alpha\delta} \delta_{\beta\gamma}. \quad (5)$$

Note that one has to properly symmetrize when using the Voigt notation, e.g.,  $C_{12}^{(\text{Voigt})} = (C_{1212} + C_{1221} + C_{2112} + C_{2121})/4$ . The originally suggested values<sup>8</sup> for  $C_{11}^{(\text{kin})}$ ,  $C_{44}^{(\text{kin})}$  and their symmetry related  $C_{ij}^{(\text{kin})}$  are in error by a factor of two. The correct values are  $C_{11}^{(\text{kin})} = Nk_B T/V$ ,  $C_{44}^{(\text{kin})} = Nk_B T/2V$ , and  $C_{12}^{(\text{kin})} = 0$ . While this kinetic contribution can usually be neglected in classical simulations, knowing the correct form is crucial for quantum systems as can be seen further below. Thus, in classical solids at non-zero temperatures, the elastic constants can be estimated as  $C_{ij} = C_{ij}^{(\text{Born})} + C_{ij}^{(\text{fluc})} + C_{ij}^{(\text{kin})}$ .

The quantum statistical formulation of the partition function of  $N$  identical particles with mass  $m$  in terms of a path-integral formulation<sup>13</sup> is given by

$$Z(N, V, T) = \lim_{P \rightarrow \infty} \lambda^{-3NP} (\beta/P) \times \int d^3 R_{11} \cdots \int d^3 R_{NP} \exp \left( -\frac{\beta}{P} V_{\text{eff}} \right) \quad (6)$$

with  $\lambda(\beta/P)$  the thermal de Broglie wavelength at temperature  $\beta/P$  and the effective potential  $V_{\text{eff}}$

$$V_{\text{eff}} = \sum_{n=1}^N \sum_{t=1}^P \left\{ \frac{m}{2} \left( \frac{\vec{R}_{it} - \vec{R}_{it+1}}{\beta\hbar/P} \right)^2 + \sum_{n' > n} V_{\text{pot}}(R_{nn't}) \right\}. \quad (7)$$

Here, the coordinate of particle  $n$  at ‘‘Trotter time’’  $t$  is denoted as  $\vec{R}_{nt}$  and  $R_{nn't}$  denotes the distance between particle  $n$  and  $n'$  at ‘‘Trotter time’’  $t$ . If exchange effects are neglected, one quantum point particle is represented as a closed classical ring polymer with the boundary condition  $\vec{R}_{nt} = \vec{R}_{n,t+P}$ . The temperature at which the simulation of the representation of the quantum particles is done is  $PT$ . Strictly speaking, the quantum limit is only obtained for infinite large Trotter numbers  $P$ , however, for practical purposes, it is usually sufficient to choose  $PT$  in the order of two times the Debye temperature.

In the following, it is convenient to represent the position of the particles in reduced dimensionless variables  $\vec{r}_{nt}$  and a (symmetric) matrix  $h_{\alpha\beta}$  that contains the shape and the size of the simulation cell such that

$$R_{nt\alpha} = \sum_{\beta=1}^3 h_{\alpha\beta} r_{nt\beta} \quad (8)$$

with  $0 \leq r_{nt\alpha} < 1$  and  $V = \det \mathbf{h}$ . Spatial periodic boundary conditions are applied by subtracting or adding unity to  $r_{nt\alpha}$  once a molecular dynamics step has moved  $r_{nt\alpha}$  out of the allowed range. With this transformation, the integration over  $\int d^3 R_{11} \cdots \int d^3 R_{NP}$  in Eq. (6) can be replaced with the expression  $V^{NP} \int d^3 r_{11} \cdots \int d^3 r_{NP}$ .

This makes it possible to take the derivative of  $\ln Z(N, V, T)$  with respect to the strain  $\epsilon_i$ . If we do not use the Voigt notation, a (virtual) variation in the stress tensor  $\delta\epsilon_{\alpha\beta}$  can be expressed as

$$\delta\epsilon_{\alpha\beta} = \frac{1}{2} \sum_{\gamma=1}^3 \left\{ (\mathbf{h}^{-1})_{\alpha\gamma} \delta h_{\gamma\beta} + (\mathbf{h}^{-1})_{\gamma\beta} \delta h_{\alpha\gamma} \right\}. \quad (9)$$

Combining Eq. (2) with Eqs. (6) through (9) then results in contributions to the elastic constants that resemble those obtained for classical systems. In particular,  $V_{\text{pot}}$  in Eqs. (1) and (3) has to be replaced with  $V_{\text{eff}}/P$ , and the factor  $Nk_B T$  in Eqs. 4 and 5 has to be replaced with  $Nk_B T P$ .

If elastic constants are evaluated in an  $NpT$  ensemble use can be made of the relation

$$\langle \delta\epsilon_{\alpha\beta} \delta\epsilon_{\beta\gamma} \rangle = (k_B T / V) (\mathbf{C}^{-1})_{\alpha\beta, \gamma\delta} \quad (10)$$

where  $\mathbf{C}$  has to be represented as a  $6 \times 6$  matrix, where we again return to the Voigt notation.

## B. Application to Ideal Gas

In order to discuss the expected statistical errors, it is helpful to consider different contributions to the elastic constants. In order to do this, we split the effective potential  $V_{\text{eff}}$  into two parts, the real potential  $V_{\text{pot}}$  and the remaining part of the right hand side of Eq. (7), which we call  $V_q$ . The terms contributing to  $C_{ij}$  can then be decomposed into the Born contribution  $C_{ij}^{(\text{Born})}$ , a term  $C_{ij}^{(\text{Born-q})}$ , which is obtained by replacing  $V_{\text{pot}}$  in the definition of  $C_{ij}^{(\text{Born})}$  with  $V_q$ , the term associated with the fluctuations of the generalized stress  $C_{ij}^{(\text{fluc})}$ , a similarly defined term  $C_{ij}^{(\text{fluc-q})}$  stemming from fluctuations of  $\partial V_q / \partial \epsilon_i$ , the cross correlation  $C_{ij}^{(\text{cross})}$  between the two terms  $\partial V_q / \partial \epsilon_i$  and  $\partial V_{\text{pot}} / \partial \epsilon_j$ , and the kinetic contribution  $C_{ij}^{(\text{kin})}$ .

$$C_{ij} = C_{ij}^{(\text{Born})} + C_{ij}^{(\text{Born-q})} + C_{ij}^{(\text{fluc})} + C_{ij}^{(\text{fluc-q})} + C_{ij}^{(\text{cross})} + C_{ij}^{(\text{kin})} \quad (11)$$

All terms related to  $V_q$  increase linearly in  $P$  in leading order as one can show in a particularly compact form if we exploit the harmonic character of the springs in the ‘‘ring polymers’’, by introducing appropriate normal coordinates

$$\tilde{R}_{nq\alpha} = \frac{1}{\sqrt{P}} \sum_{t=1}^P R_{nt\alpha} e^{2\pi i t q / P}, \quad (12)$$

so that  $V_q$  is diagonal in  $\tilde{R}_{nq\alpha}$

$$V_q = \frac{1}{2} \sum_{n=1}^N \sum_{\alpha=1}^3 \sum_{q=1}^{P-1} k_q \tilde{R}_{nq\alpha} \tilde{R}_{nq\alpha}^* \quad (13)$$

with  $k_q = 4m \sin^2(\pi q / P) / (\beta \hbar / P)^2$ .

For the ideal gas we obtain:

$$VC_{\alpha\beta\gamma\delta}^{(\text{kin})} = \frac{1}{2} N k_B T P \delta_{\alpha\delta} \delta_{\beta\gamma} \quad (14)$$

$$VC_{\alpha\beta\gamma\delta}^{(\text{Born-q})} = N k_B T (P-1) \delta_{\alpha\gamma} \delta_{\beta\delta} \quad (15)$$

$$VC_{\alpha\beta\gamma\delta}^{(\text{fluc-q})} = -2 N k_B T (P-1) \delta_{\alpha\gamma} \delta_{\beta\delta}, \quad (16)$$

while the estimator in the presence of a non-vanishing potential have the form

$$VC_{\alpha\beta\gamma\delta}^{(\text{kin})} = \frac{1}{2P} \delta_{\alpha\delta} \sum_{nt} m \dot{R}_{nt\beta} \dot{R}_{nt\gamma} \quad (17)$$

$$VC_{\alpha\beta\gamma\delta}^{(\text{Born-q})} = \frac{1}{2P} \delta_{\alpha\gamma} \sum_{it} k \delta R_{nt\beta} \delta R_{nt\delta} \quad (18)$$

$$VC_{\alpha\beta\gamma\delta}^{(\text{fluc-q})} = -2 N k_B T (P-1) \delta_{\alpha\gamma} \delta_{\beta\delta}, \quad (19)$$

with  $\delta R_{nt\alpha} = R_{nt\alpha} - R_{nt+1\alpha}$ .

In the presence of a non-vanishing  $V_{\text{pot}}$ , the individual terms will only be effected slightly, because in the quantum limit, changes in the interaction potential are much smoother than the energy changes due to changes in  $V_q$ . The net and properly symmetrized  $C_{ij}$ , however, do have well-defined values in the limit  $P \rightarrow \infty$ , which are, of course, sensitive to the interaction potential  $V_{\text{pot}}$ . For the ideal gas, the symmetrized results are listed in Table I. In a numerical calculation, it clearly will be a problem that individual terms in Eqs. (14-18) are of order  $P \gg 1$  while the final result is of order unity.

## C. Improved Primitive Estimators in PIMD

Here, we want to suggest how one can easily improve on the statistical properties of so-called primitive estimators in PIMD simulations. As a first step we define a function  $\delta K_{\alpha\beta}$  which measures how far the averaged tensor of the kinetic energy deviates from its expectation value

$$\delta K_{\alpha\beta} = \frac{1}{2} \sum_{n,t} \langle \tilde{m}_{nt} v_{n\alpha} v_{n\beta} \rangle_{\text{simul}} - \frac{1}{2} N k_B T P^2 \delta_{\alpha\beta}, \quad (20)$$

where  $\tilde{m}_{it}$  represents the (kinetic) mass of particle  $n$  at Trotter time  $t$  (note that kinetic masses can be chosen arbitrarily independent of the physical mass<sup>6</sup>) and  $v_{i\alpha}$  is the  $\alpha$  component of its velocity.  $\langle \bullet \rangle_{\text{simul}}$  symbolizes an expectation value obtained in a simulation. Ideally,  $\delta K_{\alpha\beta}$  would be zero, but, due to finite statistics, finite time-steps, and other round-off errors, we will usually find  $\delta K_{\alpha\beta} \neq 0$ . It is very likely that this deviation  $\delta K_{\alpha\beta}$  will convert into a similarly large deviation in potential energy, in particular into  $V_q$  for large Trotter numbers  $P$ .

At large  $P$ , the external potential is locally only a small perturbation to the springs connecting neighbored beads on the ring. Due to the conversion of kinetic energy to potential energy, similar deviations from the exact thermodynamic average can be expected in  $V_q$ . This makes it possible to define an optimized estimator for quantities associated with  $V_q$ , namely

$$\frac{1}{2} \sum_n \sum_t \frac{mP^2}{\beta\hbar} \langle \delta R_{nt\alpha} \delta R_{nt\beta} \rangle_{\text{optim.}} = \frac{1}{2} \sum_n \sum_t \frac{mP^2}{\beta\hbar} \langle \delta R_{nt\alpha} \delta R_{nt\beta} \rangle_{\text{simul.}} - \delta K_{\alpha\beta} \quad (21)$$

Similar correction terms can easily be generalized to higher orders, e.g. deviations of  $\langle \tilde{m}_{it}^2 v_{i\alpha} v_{i\beta} v_{i\gamma} v_{i\delta} \rangle_{\text{simu.}}$  from its thermal expectation value can be expected to convert into  $\langle (mP^2/\beta\hbar)^2 \delta R_{i\alpha} \delta R_{i\beta} \delta R_{i\gamma} \delta R_{i\delta} \rangle_{\text{simu.}}$

In passing we want to explicitly give the improved estimator for the kinetic energy, which can be used in PIMD. It is similar to the so-called primitive estimator<sup>11</sup>, but the expression  $3Nk_B TP/2$  arising in the original estimator is replaced by the actual average net kinetic energy. With the quantities introduced in Eq. (11), the average kinetic energy may simply be expressed as

$$\langle T_{\text{kin}} \rangle = V \sum_{\alpha=1}^3 \left( C_{\alpha\alpha\alpha}^{(\text{kin})} - C_{\alpha\alpha\alpha}^{(\text{born-q})} \right) \quad (22)$$

As outlined above, the new primitive estimator benefits from the correlation of kinetic and potential energy in the isomorphic classical representation. This is demonstrated in Fig. 1, where the average statistical deviation from terms of the type  $C_{1111}$  are shown.

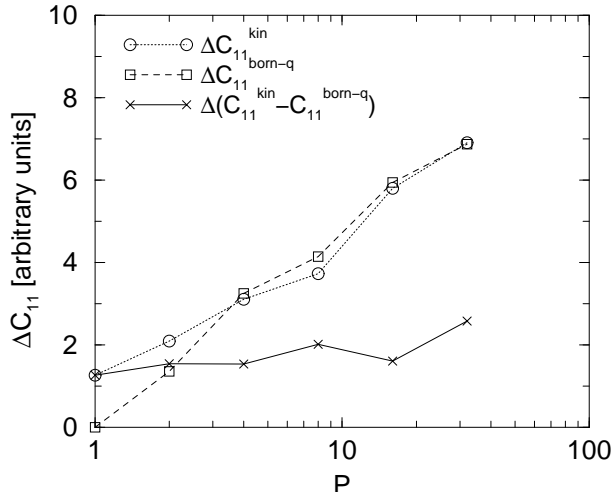


FIG. 1. Statistical variances of the components  $C^{(\text{kin})}$  and  $C^{(\text{Born-q})}$  for various Trotter numbers  $P$ . Similar conditions like same number of MD steps, same temperature, etc. have been used for all calculations.

Note that the statistical error of  $\Delta C_{11}^{(\text{Born-q})}$ , which is identical to the statistical error of the original primitive estimator, increases much slower than the statistical error of the primitive estimator when examined originally<sup>11</sup>. This is due to the development of efficient sampling methods in the meantime<sup>6</sup> which suppress slowing down with increasing  $P$ . The new estimator has a strongly reduced statistical noise as compared to the original one, yet, results in the correct expectation value. Furthermore, using larger time steps than in our production runs, we have noticed that systematic errors due to finite-time steps, are considerably reduced as well with the new estimator. We want to note that in later production runs for strongly quantum mechanical systems such as solid  $^3\text{He}$ , statistical error bars obtained with the new estimators are as small as statistical error bars associated with the so-called virial estimator<sup>11</sup>.

#### D. Elastic Constants Under Pressure

Care has to be taken when discussing elastic constants of systems under pressure, because their definition is not unique.<sup>14</sup> One commonly distinguishes between the so-called Birch coefficients  $B_{ij}$  and the elastic constants  $C_{ij}$ . They are defined as the second derivative of the free energy with respect to the Lagrangian strain and the “regular” strain, respectively. The relation between  $B_{ij}$  and  $C_{ij}$  merely depend on the externally applied stress but not on the symmetry of the crystal. In the case of hydrostatic pressure, the relations are given by<sup>14</sup>

$$B_{ij} = C_{ij} + \Delta_{ij} \quad (23)$$

with  $\Delta_{ii} = -p$  for  $1 \leq i \leq 6$ ,  $\Delta_{ij} = +p$  for  $i \leq 3$  and  $j \leq 3$  with  $i \neq j$ , and zero else.

The generalization of our previous estimator of  $C_{ij}$  to the non-zero pressure case are as follows: Evaluation of the strain fluctuations as indicated in Eq. 10 result in the Birch coefficients, while the formula given for zero-pressure  $C_{ij}$  in the  $NVT$  ensemble enable us to calculate the  $C_{ij}$  at non-zero pressures.

Note that the proper stability criterion for solids under pressure is a positive definite matrix of Birch coefficients rather than a positive definite matrix of elastic constants.<sup>15</sup> It is important to keep in mind that symmetry relations of  $C_{ij}$  which are obtained under the assumption of short-ranged two-body potentials are not valid for  $B_{ij}$  in the case of any non-zero externally applied stress.<sup>14</sup>

#### E. Simulation Method

Simulations are carried out in both, the  $NpT$  and the  $NVT$  ensemble. Molecular dynamics are favorable over Monte Carlo simulations in the constant stress ensemble ( $NpT$ ), because all variables are averaged simultaneously - in particular all elements of the strain tensor.

In order to keep the externally applied stress tensor constant, the Parrinello-Rahman method<sup>16</sup> has been applied to the classical representation which is isomorphic to the quantum system. The classical representation is defined by Eqs. (6) and (7). More details are given elsewhere<sup>17</sup> on how to efficiently collapse the time-scales associated with the different motions of the system such as the intramolecular breathing of the closed classical ring representing the quantum point particle, the center-of-mass motion of the ring, and the fluctuations of the cell geometry.

### III. APPLICATIONS

#### A. Argon

Argon is a convenient test case for the calculation of quantum-mechanical elastic constants, because it lies in between what is considered a quantum solid like solid helium under pressure, and what is considered a “classical” solid like solid Xenon. For the Argon test-case, we intend to determine the shift of the quantum mechanical elastic constants with respect to the classical elastic constants and the relative importance of the individual contributions to the net result. The results will be an indicator for what we can expect from the quantum mechanical shift in the elastic constants of other solids.

First, we compare classical to quantum mechanical calculations in Fig. 2, where results in the  $NpT$  and the  $NVT$  ensemble are shown. In the simulations of Argon, a Lennard Jones potential  $V = 4\epsilon[(\sigma/r)^{12} - (\sigma/r)^6]$  was used with parameters  $\epsilon = 1.67 \times 10^{-21}$  J and  $\sigma = 3.405$  Å. All simulations were based on system sizes  $N = 500$  and statistics of  $5 \times 10^5$  time steps. The Trotter number in the quantum runs has been chosen such that  $PT = 120$ . Increasing  $P$  any further does not change the results within the statistical error bars.

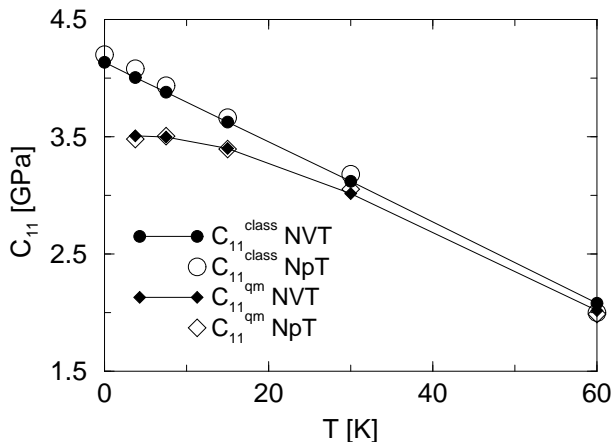


FIG. 2. Elastic constant  $C_{11}$  of solid Argon at ambient pressure as a function of temperature  $T$ . Classical and quantum simulations were carried out at constant volume  $V$  and constant external stress.

In Fig. 2, it can be seen that there is a considerable discrepancy between classical and quantum mechanical elastic constants. The quantum  $C_{11}$  levels at about  $T = 15$  K and one may extrapolate  $C_{11} \approx 3.5$  GPa for the quantum mechanical ground state, while classically,  $C_{11} \approx 4.2$  GPa at zero temperature. The relative effects in  $C_{12}$  and  $C_{44}$  are similar. Note that this effect of a  $\mathcal{O}(20\%)$  reduction in  $C_{11}$  is considerably larger than the increase in the lattice constant of about 1% or the decrease of 10% of the heat of formation.

The bulk of the reduction in  $C_{11}$  does not stem from the expressions introduced in Sec. II A. There are two important contributions, namely the Born term and the term related to the fluctuation of the Lennard Jones potential. Details are given in Table II. The classical system at  $T = 0$  K has only one non-zero contribution, namely  $C_{11}^{(\text{Born})} = 4.2$  GPa. As expected, differences between classical and quantum results become negligible as the temperature approaches (or surpasses) the Debye temperature, which in the case of Argon is  $T_D = 93$  K.

#### B. Helium

While Argon shows significant differences between classical and quantum mechanical elastic constants, the corrections due to the kinetic energies are fairly small. Helium, in particular  $^3\text{He}$ , is much more “quantum” than Argon and therefore a more challenging test case than Argon. The solid forms of  $^3\text{He}$  are only stable under pressure.<sup>18</sup> Hence, we have to distinguish between elastic constants and Birch coefficients. There are three different, stable  $^3\text{He}$  lattice structures: the bcc phase is mostly stable in the interval  $0 \leq T \leq 2$  K at pressures  $3 \text{ MPa} \leq p \leq 10 \text{ MPa}$ , hcp is the stable low-temperature phase at pressures  $p > 10 \text{ MPa}$ , and there is a small temperature regime at pressures  $p > 150 \text{ MPa}$  where a stable fcc phase is found in between the hcp and the fluid phase.

The simulations for helium are all based on the Aziz potential<sup>19</sup>, which is known to be fairly reliable up to moderate pressures. Exchange effects are neglected. In the temperature regime accessible to our simulation they are generally believed to be unimportant. The transition to a long-range ferromagnetic and antiferromagnetic transitions in hcp and bcc  $^3\text{He}$ , respectively, only take place at temperatures in the mK regime.

##### 1. fcc $^3\text{He}$

In this subsection, we will focus on one particular representative point in the stable fcc phase, because it is computationally very demanding to calculate elastic constants. In order to be able to work with relatively small Trotter numbers, it is necessary to go to large temperatures and low pressures. Yet, we want to avoid to be too

close to a phase transition, e.g., the fcc fluid phase transition. The combination of  $T = 18$  K and  $p = 200$  MPa seems to be an appropriate choice: The quantum limit is basically reached with Trotter number  $P = 32$  and the transition to the fluid phase takes place at sufficiently higher temperature, namely at  $T = 22$  K. Although the thermodynamic stability field of the hcp phase is located at temperatures  $T < 18$  K for the applied pressure, one may certainly expect metastability of the fcc phase in the time window accessible to our simulations.

The different  $C_{ij}$  along with their individual contributions are listed in Table III. It is interesting to note that the Cauchy relation  $C_{12} = C_{44}$  for cubic crystals with central potentials basically also hold for the quantum solid, e.g.,  $C_{44}/C_{12} \approx 0.95$ , while the Birch coefficients don't:  $B_{44}/B_{12} \approx 0.50$ . See Sec. IID for the definition and the relevance of Birch coefficients. It is instructive to represent the individual contributions to  $C_{11}$  graphically, which is done in Fig. 3. It is noticeable that the sum of the corrections to  $C_{11}$  which are related to the kinetic energy is relatively small, while the individual contributions are fairly large. Yet, the solid is far away from being classical. The kinetic energy of  ${}^3\text{He}$  is about  $88.9 k_B\text{K}$ , which is considerably larger than the thermal classical energy of  $1.5 k_B \times 18 \text{ K} = 27 k_B\text{K}$ , thus  $T/T_{\text{Debye}} < 0.3$ . ‘‘Classical’’ helium would have  $C_{11} = 1.63$  GPa at the same external temperature and pressure. From Fig. 3 we can see that it is possible to approximate the elastic constants fairly reasonably if only the Born contribution and the contribution due to the fluctuating real potential are included into the calculation.

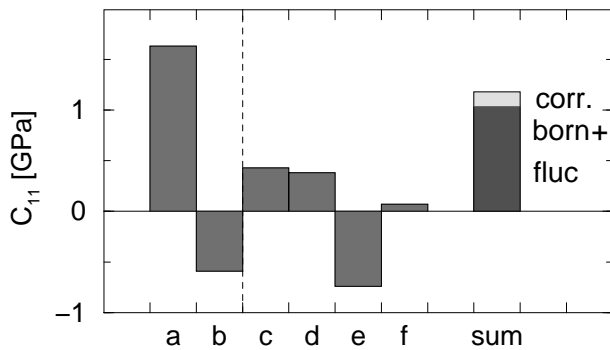


FIG. 3. Individual contributions to  $C_{11}$  of fcc  ${}^3\text{He}$  at pressure  $p = 200$  MPa and temperature  $T = 18$  K. a: Born, b: fluc, c: kin, d: Born-q, e: fluc-q, f: cross; corr. summarizes c, d, e, and f. Trotter Number  $P = 32$  and number of particles  $N = 500$ .

## 2. bcc ${}^3\text{He}$

The bcc phase can be considered to be the most interesting solid helium phase, because it is classically unstable. fcc and hcp phase can both be considered to be classically stable at low temperatures, because their free energy differences are small. An interesting phenomena

in the (quantum mechanical) bcc phase is the radial distribution function  $g(r)$ : The peaks in  $g(r)$  can not easily be related to nearest neighbors, next neighbors, etc., but the contributions of different neighboring shells ‘‘group’’ together. This is shown in Fig. 4. The final  $g(r)$  can be interpreted as a sum of broadened individual lines, which are represented in Fig. 4 as well. The overlap of such broadened lines is accompanied by a strong diffusion of individual atoms. We did not investigate in depth this diffusion process.

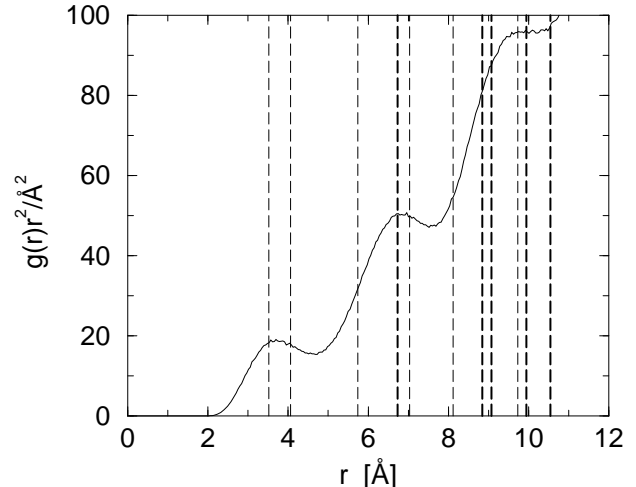


FIG. 4. Radial distribution function  $g(r)$  times  $r^2$  as a function of distance  $r$  for bcc  ${}^3\text{He}$  at  $T = 2$  K and  $P = 10$  MPa. The broken lines indicate the distance of nearest neighbors, next neighbors, etc. The width of the broken lines is proportional to the number of atoms in each shell.

In the case of  ${}^3\text{He}$ , some experimental data is available for the elastic constants or Birch coefficients. In Fig. 5, we compare the  $B_{ij}$  calculated in our study with the available experimental data and some theoretical predictions. Simulations at three different combinations of pressures and temperatures were performed:  $p_1 = 10$  MPa with  $T_1 = 2$  K,  $p_2 = 7$  MPa with  $T_2 = 1.5$  K, and  $p_3 = 4$  MPa with  $T_3 = 1$  K. In all cases, Trotter numbers of  $P = 256$  were found to reflect the quantum limit sufficiently well, and the particle number was  $N = 432$ . The elastic constants can be assumed to be mainly temperature independent, as the temperatures are far below the Debye temperatures, e.g., the ratios  $q_i = \langle T_{\text{kin}} \rangle / 1.5 k_B T$  which are close to unity at the Debye temperature turned out to be:  $q_1 = 10.27$ ,  $q_2 = 12.22$ , and  $q_3 = 15.4$ .

For bcc  ${}^3\text{He}$ , the (relative) corrections in  $C_{ij}$  which are related to the kinetic energy are much larger than in fcc  ${}^3\text{He}$ . This can be seen in Table IV: the corrections make up nearly 80% of the total  $C_{11}$  for a pressure  $p = 4$  MPa and about 30% for a pressure of  $p = 10$  Pa (not explicitly shown in Tables). We want to note that the elastic constants obtained in the  $NVT$  ensemble and in the  $NpT$  ensemble agreed within the statistical error bars.

hcp  $^3\text{He}$  has more independent elastic constants than bcc and fcc  $^3\text{He}$ , respectively. The trend in all elastic constants, however, is yet again the same as in bcc or fcc helium: the larger the pressure the more dominant the “classical” contribution to the elastic constants. Note that on the other hand, the absolute corrections due to the kinetic energy increase with increasing pressure. Details of the calculations are given in Tables V-VI. Note that the classical elastic constants would be nearly three times as large as the quantum mechanical elastic constants at a pressure  $p = 90$  MPa and even more than seven times as large in the case of  $p = 15$  MPa. Due to the good agreement with the experimentally measured bulk modulus, see Fig. 5, one may expect our quantum mechanical data to be fairly accurate. To our knowledge, the values presented in Tables V-VI are predictions. No theoretical or experimental data is known to us.

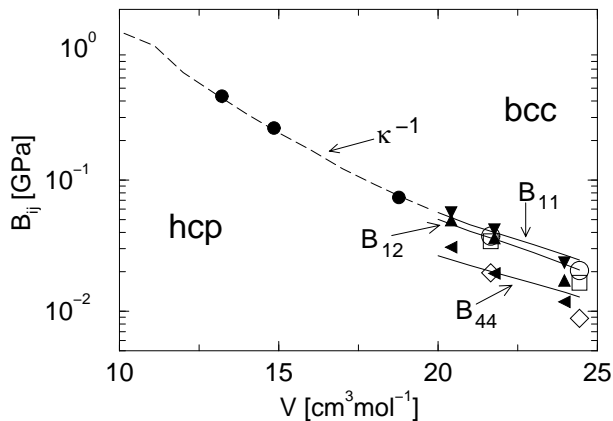


FIG. 5. Birch coefficients for bcc  $^3\text{He}$  (right hand side) and bulk modulus for hcp  $^3\text{He}$  (left hand side) as a function of the molar volume. All filled symbols refer to this work. The broken line represents experimental data from Ref. [20]. The solid lines represent theoretical predictions from Ref. [21]. Open symbols refer to experimental data from Ref. [22].

### C. Kinetic energy of solid $^3\text{He}$

The calculation and measurement of kinetic energies  $\langle T_{\text{kin}} \rangle$  in condensed helium phases has attracted a lot of recent attention. Condensed helium is highly quantum mechanical and therefore provides an ideal test ground for the application of many-body quantum statistical theories. Recent experimental developments have made it possible to measure kinetic energies with great accuracy and thus provide important tests on the theories.

The data for  $\langle T_{\text{kin}} \rangle$  presented in this study complement data by Draeger and Ceperley, which has been presented recently<sup>23</sup>. In particular, data for the bcc phase and the low-pressure hcp regime are presented,

see Fig. 6. We would like to emphasize that in both studies relatively high temperatures were taken in the high-pressure regime with small average atomic volume of  $V < 20 \text{ \AA}^3$ , e.g., the ratio of kinetic energy to thermal energy,  $q = 2\langle T_{\text{kin}} \rangle / 3k_B T$  is only slightly larger than three. Of course, this is still well below the Debye temperature, but some thermal activation will be present.

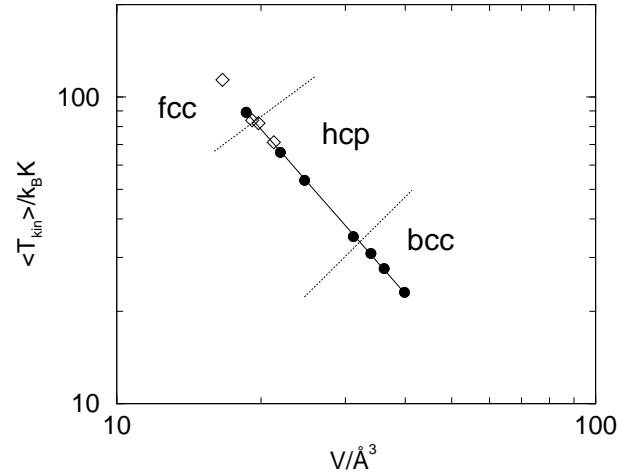


FIG. 6. Thermal kinetic energy  $\langle T_{\text{kin}} \rangle$  as a function of the average volume per atom. Open diamonds are values from PIMC simulations by Draeger and Ceperley. The straight line is a power law fit to our data.

Our data can be very well fit with an expression of the type

$$\langle T_{\text{kin}} \rangle = AV^{-\alpha}, \quad (24)$$

where  $A$  and  $\alpha$  are fit parameters.  $A$  and  $\alpha$  turn out to be  $\alpha \approx 1.78$  and  $A = 16100$  if  $V$  is expressed in  $\text{\AA}^3$  per atom and kinetic energies in units of  $k_B K$ . Within the regime considered here, our data is reflected within 1.5% accuracy. In the bcc phase, this fit underestimated  $\langle T_{\text{kin}} \rangle$  by about 1.5%, in the hcp phase,  $\langle T_{\text{kin}} \rangle$  is slightly overestimated. The value of  $\langle T_{\text{kin}} \rangle$  near the quantum mechanical ground state seems to be mainly a function of the molar or atomic volume only - relatively insensitive to the actual crystalline phase.

We want to emphasize that the data points in Fig. 6 which turn out to be larger than the values suggested by the fit, all have relatively small values of the quantum parameter  $q$ . Thus, going to even smaller values of  $q$ , which is computationally expensive, might even increase the quality of the fit. Omitting all data with  $q < 5$ , an exponent of  $\alpha = 1.75$  is found. It is quite surprising that the birch coefficients depend exponentially on the molar volume (Fig. 5), the quantum mechanical ground state kinetic energy, however, only changes algebraically with  $V$ .

#### IV. CONCLUSIONS

Expressions for the elastic constants of quantum solids have been presented in terms of a path integral representation in the  $NVT$ -ensemble. These expressions have then been applied and proven useful in path integral molecular dynamics simulations of solid Argon and hcp, fcc, and bcc helium III. In the  $NpT$  ensemble, the classical formula can be used which relates strain fluctuations with elastic constants or - in the case of non-zero external pressure - with Birch coefficients. With the exception of hcp and bcc  $^3\text{He}$ , the  $NVT$  expressions were dominated by the terms which one knows from classical simulations: the Born term and the potential fluctuation term. In the case of bcc  $^3\text{He}$ , terms related to the kinetic energy dominate the elastic constants.

The quantum mechanical motion of the particles shows a stronger effect on the elastic constants than one might expect. E.g., in the case of Argon at zero external pressure, the quantum mechanical  $C_{11}$  is reduced by about 20%, while cohesion energy and lattice constants are only decreased by 10% and increased by 1%, respectively. Hence, in order to have truly accurate estimates for elastic constants from computer simulations, quantum effects need to be taken into consideration.

While deriving the expressions for elastic constants, an improved primitive estimator for the kinetic energy has been proposed. The statistical uncertainties of this estimator do not increase with increasing Trotter number. Due to short correlation times, the improved primitive estimator results in statistical error bars smaller but in the order of the virial estimator for highly quantum systems such as solid  $^3\text{He}$ . However, unlike the virial estimator, the improved primitive estimator can only be used in path integral molecular dynamics, but not in Monte Carlo simulations.

#### ACKNOWLEDGMENTS

We thank Kurt Binder for useful discussions. Support from the BMBF through Grant 03N6015 and from the Materialwissenschaftliche Forschungszentrum Rheinland-Pfalz is gratefully acknowledged.

- <sup>1</sup> N. W. Ashcroft and N. D. Mermin, *Solid State Physics* (Saunders College, Philadelphia, 1976).
- <sup>2</sup> B. J. Berne and D. Thirumalai, *Annu. Rev. Phys. Chem.* **37**, 401 (1986).
- <sup>3</sup> K. E. Schmidt and D. M. Ceperley, in *The Monte Carlo Method in Condensed Matter Physics*, edited by K. Binder (Springer-Verlag, Berlin, 1995).
- <sup>4</sup> C. Chakravarty, *Int. Rev. Phys. Chem. Solids* **16**, 421 (1997).
- <sup>5</sup> D. Marx and M. H. Müser, *J. Phys.: Condens. Matter* **11**, R117-R155 (1999).
- <sup>6</sup> M. E. Tuckerman, B. J. Berne, G. J. Martyna, and M. L. Klein, *J. Chem. Phys.* **99**, 2796 (1993).
- <sup>7</sup> M. E. Tuckerman and A. Hughes, in *Classical and Quantum Dynamics in Condensed Phase Simulations* (World Scientific, Singapore, 1998).
- <sup>8</sup> D. R. Squire, A. C. Holt, and W. G. Hoover, *Physica* **42**, 388 (1969).
- <sup>9</sup> M. Parrinello and A. Rahman, *J. Chem. Phys.* **76**, 2662 (1982).
- <sup>10</sup> M. Sprik, R. W. Impey, and M. L. Klein, *Phys. Rev. B* **29**, 4368 (1984).
- <sup>11</sup> M. F. Herman, E. J. Bruskin, and B. J. Berne, *J. Chem. Phys.* **76**, 5150 (1982).
- <sup>12</sup> We use the symbol  $C_{ij}$  for elastic constants in the Voigt notation and  $C_{\alpha\beta\gamma\delta}$  for elastic constants in the tensor notation.
- <sup>13</sup> R. P. Feynman and A. R. Hibbs, *Quantum Mechanics and Path Integrals*, (Mc.Graw-Hill, New York, 1965).
- <sup>14</sup> D. C. Wallace, in *Solid State Physics* **25**, ed. H. Ehrenreich, F. Seitz, and D. Turnbull (Academic Press, New York, 1971); *Thermodynamics of Crystals* (Wiley, New York, 1972).
- <sup>15</sup> J. Wang, S. Yip, S. R. Phillpot, and D. Wolf, *Phys. Rev. Lett.* **71**, 4182 (1993).
- <sup>16</sup> M. Parrinello and A. Rahman, *J. Appl. Phys.* **52**, 7182(1981).
- <sup>17</sup> M. H. Müser, to be published.
- <sup>18</sup> E. R. Dobbs, *Solid Helium Three*, (Oxford University Press, Oxford, 1994).
- <sup>19</sup> R. A. Aziz, F. R. W. Court, and C. C. K. Wong, *Mol. Phys.* **61**, 1487 (1987).
- <sup>20</sup> C. A. Swenson, in *Rare gas solids*, ed. M. L. Klein and J. A. Venables (Academic Press, London).
- <sup>21</sup> H. R. Glyde and F. C. Khanna, *Can. J. Phys.* **49**, 2997 (1971).
- <sup>22</sup> D. S. Greywall, *Phys. Rev. B* **11**, 1070 (1975).
- <sup>23</sup> E. W. Draeger and D. M. Ceperley, *Phys. Rev. B* **61**, 12094 (2000).

	kin	Born-q	fluc-q	sum
$C_{11}$	P	P-1	-2(P-1)	1
$C_{12}$	0	0	0	0
$C_{44}$	P/2	(P-1)/2	-(P-1)	1/2

TABLE I. Individual components of  $C_{ij}$  for the ideal gas in units of  $Nk_B T/V$  in the path integral representation.



	Born	fluc	kin	Born-q	fluc-q	cross	corr	sum
quantum	3.72639	-0.30566	0.04337	0.03278	-0.05530	0.05469	0.07555	3.49627
	0.00005	0.00156	0.00001	0.00001	0.00053	0.00150	0.00137	0.00195
class.	4.03116	-0.15535	0.00278	0	0	0	0.00278	3.87860
	0.00004	0.00107	0.00001				0.00001	0.00107

TABLE II. Individual contributions to  $C_{11}$  for Argon at  $T = 7.5$  K for the quantum and the classical calculation. Lower rows give statistical uncertainties based on 500.000 molecular dynamics steps. The individual contributions are introduced in Eq. (11). The colon named “corr” summarizes all corrections involving contributions from the kinetic energy: kin, Born-q, fluc-q, and cross.

	Born	fluc	kin	Born-q	fluc-q	cross	corr	sum
$C_{11}$	1.63	-0.59	0.43	0.38	-0.74	0.07	0.14	1.18
$C_{12}$	0.77	-0.24	0	0	0.01	0.12	0.13	0.66
$C_{44}$	0.77	-0.23	0.21	0.19	-0.36	0.05	0.09	0.63

TABLE III. Individual contributions to  $C_{ij}$  for fcc  $^3\text{He}$  at  $T = 18$  K and pressure  $p = 200$  MPa. The colon named “corr” summarizes same terms as in previous table. Statistical error bars of final  $C_{ij}$  are smaller than 5%.

	Born	fluc	kin	Born-q	fluc-q	cross	corr	sum
$C_{11}$	87.00	-79.15	88.59	83.27	-152.96	8.26	27.16	35.00
$C_{12}$	35.19	-29.47	0	0	4.84	16.44	21.28	27.00
$C_{44}$	35.19	-27.84	44.28	41.62	-78.53	0.61	7.98	15.33

TABLE IV. Individual contributions to  $C_{ij}$  for bcc  $^3\text{He}$  at  $T = 2$  K and pressure  $p = 4$  MPa. The colon named “corr” summarizes same terms as in previous table. Statistical error bars of final  $C_{ij}$  are smaller than 10%.

$p$	$T/\text{K}$	$C_{11}$	$C_{12}$	$C_{13}$	$C_{33}$	$C_{44}$	$C_{66}$	$\langle V \rangle / \text{cm}^3$
0.09	10.0	0.701	0.303	0.193	0.822	0.206	0.193	13.22
0.05	5.0	0.405	0.172	0.111	0.492	0.123	0.108	14.85
0.015	2.5	0.118	0.052	0.034	0.144	0.039	0.032	18.77

TABLE V. Independent elastic constants of hcp- $^3\text{He}$  as obtained in the  $NpT$  ensemble. The thermal expectation value of the molar volume  $\langle V \rangle$  is inserted as well. Pressure and elastic constants are expressed in GPa. Statistical error bars of  $C_{ij}$  are smaller than 5%.

$V/\text{cm}^3$	$T/\text{K}$	$C_{11}$	$C_{12}$	$C_{13}$	$C_{33}$	$C_{44}$	$C_{66}$	$\langle p \rangle$
13.22	10.0	0.700	0.234	0.208	0.810	0.169	0.192	0.090
14.85	5.0	0.407	0.183	0.125	0.447	0.138	0.120	0.050
18.77	2.5	0.135	0.043	0.039	0.156	0.036	0.025	0.015

TABLE VI. Independent elastic constants of hcp- $^3\text{He}$  as obtained in the  $NVT$  ensemble. The thermal expectation value for the pressure  $\langle p \rangle$  is inserted as well.  $p$  and  $C_{ij}$  are expressed in GPa.